

LEDGF/p75 is Dispensable for Hematopoiesis but Essential for MLL-rearranged Leukemogenesis

Sara El Ashkar¹, Juerg Schwaller², Tim Pieters^{3,4}, Steven Goossens^{3,4}, Jonas Demeulemeester^{1,5}, Frauke Christ¹, Siska Van Belle¹, Sabine Juge², Nancy Boeckx^{6,7}, Alan Engelman⁸, Pieter Van Vlierberghe^{3,4}, Zeger Debyser^{1*} and Jan De Rijck^{1*}

¹Laboratory for Molecular Virology and Gene Therapy, Department of Pharmaceutical and Pharmacological Sciences, KU Leuven, Leuven, Belgium.

²Department of Biomedicine, University Children's Hospital (UKBB), University of Basel, Switzerland.

³Center for Medical Genetics, Ghent University, Ghent, Belgium.

⁴Cancer Research Institute Ghent (CRIG), Ghent, Belgium.

⁵Current address: The Francis Crick Institute, London, United Kingdom.

⁶Department of Laboratory Medicine, University Hospitals Leuven, Leuven, Belgium.

⁷Department of Oncology, KU Leuven, Leuven, Belgium

⁸Department of Cancer Immunology and AIDS, Dana-Farber Cancer Institute, Harvard Medical School, Boston, United States of America.

*Shared senior authorship.

Correspondence should be addressed to Jan De Rijck:

Laboratory for Molecular Virology and Gene Therapy

Kapucijnenvoer 33, VCTB +5

3000 Leuven, Belgium

jan.derijck@kuleuven.be, zeger.debyser@kuleuven.be

Tel.: +32 16 374038, Fax.: +32 16 336336

Supplemental Methods

Plasmids

The *pMSCV-HoxA9-pgk-neo* and *MSCV-pgk-neo* vectors were provided by Dr. Guy Sauvageau (Institute for Research in Immunology and Cancer, IRIC, Canada). The pMSCV retroviral vector encoding the *MLL-AF9* or *eGFP* and the lentiviral vector expressing *LEDGF/p75*-miRNA or *eGFP*-miRNA control were previously described¹. The transfer plasmid for miRNA-based knockdown of *Ledgf/p52* (target sequence 5'-AAGCACCAAACAACATGTAATC-3') was generated based on miRNA-R30 technology². The retroviral vectors *pMSCV-MLL-ENL-Neo* and *pMSCV-Neo* were provided by Dr. Akihiko Yokoyama (Laboratory for Malignancy Control Research, Kyoto University, Japan). To clone point mutations in the MLL-ENL construct, a NotI/MunI fragment from *pMSCV-MLL-ENL-Neo* was subcloned in a pUC backbone. Subsequently a NotI/BspEI fragment was replaced by a synthetic codon optimized sequence with a unique Pfl23II restriction site whereupon the NotI/MunI fragment was shuttled back to *pMSCV-MLL-ENL-Neo*. These mutations were then introduced by replacement of Pfl32II/NotI fragments by synthetic sequences containing the respective mutations.

Western blot

Cells were washed in phosphate-buffered saline (PBS) and cell pellets were lysed and boiled in 1% SDS. Protein samples were separated by sodium dodecyl sulfate-polyacrylamide gel electrophoresis and electroblotted onto polyvinylidene difluoride membranes (Bio-Rad). Membranes were blocked with milk powder in PBS-0.1% Tween

20 and detection was performed using specific antibodies against LEDGF/p75 (Bethyl, A300-848A) or β -tubulin (Sigma, T4026-2). Horseradish peroxidase (HRP)-conjugated secondary antibodies allowed for chemiluminescence detection (ECL+; Amersham).

Bone marrow transplantation

For reconstitution experiments, donor mice were genotyped for *Cre* expression. Recipient mice (8-10 weeks old) received a lethal irradiation dose of 8 Grays 24 hours prior to tail-vein injection of lin⁻ cells (1×10^6 cells per animal). *Psip1* excision was confirmed by qRT-PCR from blood of recipient animals 4 week post-transplantation (data not shown). For leukemogenesis studies *in vivo*, lin⁻ cells were transduced with the indicated fusion and similarly transplanted into irradiated recipients.

Quantitative RT-PCR

RNA was isolated using Aurum Total RNA mini kit (Bio-Rad). cDNA was prepared with High Capacity cDNA Reverse Transcription Kit (Thermoscientific). Each reaction contained 12.5 μ L IQ Supermix (Biorad) or LightCycler® 480 SYBR Green I Master (Roche), 200nM forward and reverse primers and 200nM probe (if indicated) in a final volume of 25 μ L. Samples were run in triplicates for 10 minutes at 95°C followed by 50 cycles of 10 seconds at 95°C and 30 seconds at 55°C in LightCycler 480 (Roche). Analysis was performed using the LightCycler 480 software supplied by the manufacturer. All primers and probes are listed in Table S1.

Chromatin immunoprecipitation

Lin- cells were freshly extracted from mice (8-10 weeks old) and fixed using 2mM Disuccinimidyl Glutarate for 30 minutes followed by 1% formaldehyde fixation for 10 minutes. 10^7 fixed cells were lysed in 120 μ L lysis buffer (1% SDS, 10mM EDTA, 50mM Tris, pH 8.1) and sonicated using a Bioruptor sonicator (Diagenode) for 40 cycles of 30 seconds with 30 seconds intervals in a water bath at 4°C. Subsequent steps were performed as described³. An MLL antibody (Bethyl laboratories, A300-086A) was used to precipitate MLL. qPCR was performed as described above. Primers are listed in Table S1. ChIP-qPCR signals were calculated as a percentage of total input³.

RNA sequencing analysis

RNA extraction was performed as described above and 1 μ g RNA was used as input. Sequencing libraries were prepared using an Illumina TruSeq Stranded mRNA Library Prep Kit according to the manufacturer's instructions. Samples were subsequently 50bp single-end sequenced on an Illumina HiSeq 2500. RNA-Seq reads were mapped to the GRCm38 mouse reference genome assembly using STAR 2.5.1b and read counts per gene (GENCODE release M8/Ensembl 83 gene annotation) were computed⁴. The R/Bioconductor package DESeq2⁵ was used for normalization and differential gene expression analysis.

For gene set enrichment analysis, mouse gene IDs were mapped to their human counterparts where possible using Ensembl BioMart. Analysis on the ranked and humanized gene list was performed with GSEA v2.0 using the Molecular Signatures Database C6 oncogenic signatures collection.

HPEAK ChIP-Seq peak calls for MLL1, WDR5 and H3K4me2 from Xu et al., *Cell Discovery*, 2016 were obtained from the NCBI's Gene Expression Omnibus (series GSE68823)⁶. Peaks were annotated and filtered using R/Bioconductor to yield a gene set which had MLL-bound promoters (i.e. an MLL ChIP-Seq peak overlapping a region of 2000bp upstream of the TSS to 200bp downstream of it). A subset of genes with evidence for MLL-complex binding to the promoter was obtained by also requiring overlap with WDR5 and H3K4me2 ChIP-Seq peaks. Both gene sets, as well as those reported for MLL-ENL⁷ or MLL-AF9⁸ targets were assessed for enrichment in the ranked gene list using GSEA v2.0.

The RNA-Seq data have been deposited in NCBI's Gene Expression Omnibus⁶ and are accessible through GEO Series accession number GSE104138 (<https://www.ncbi.nlm.nih.gov/geo/query/acc.cgi?acc=GSE104138>).

Supplemental Figures

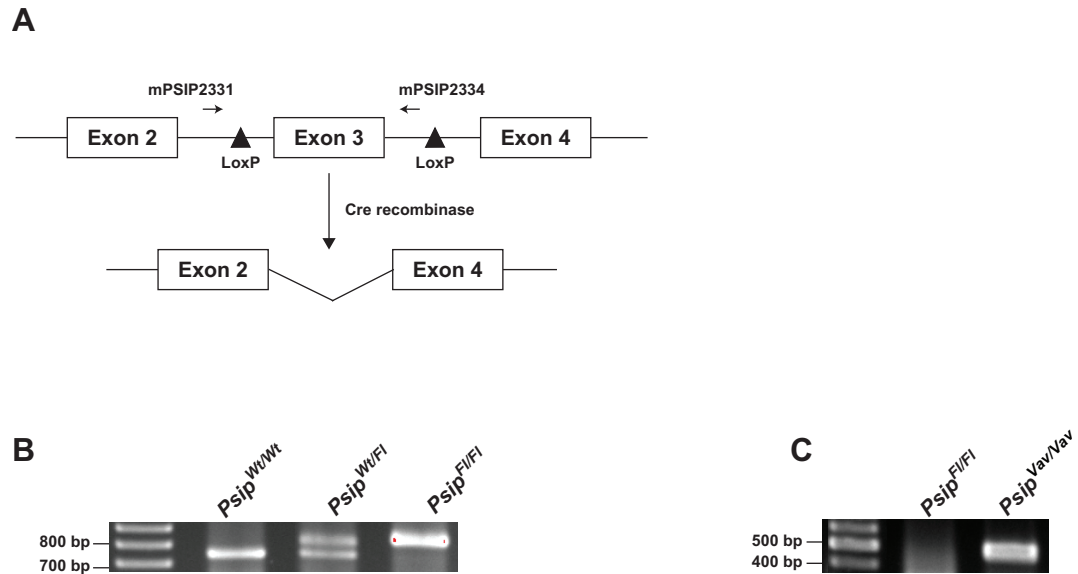


Figure S1. Generation of *Psip1* knockout mice.

(A) Schematic representation of the floxed *Psip1* (*Psip^{F1/F1}*) gene and the primers used for genotyping. LoxP sites flank exon 3, the second coding exon of *Psip1*, which is deleted after Cre recombination.

(B) Genomic DNA PCR analysis for the genotyping of *Psip^{F1/F1}* mice. mPSIP2331 and mPSIP2334 primers amplify 745 bp and 802 bp bands for the wild-type and floxed allele, respectively.

(C) Genomic DNA PCR analysis for the detection of Cre (450 bp) in *Psip^{F1/F1}* mice crossed with Vav-iCre mice (referred to as *Psip^{F1/F1} Vav-Cre* positive mice or *Psip^{Vav/Vav}*).

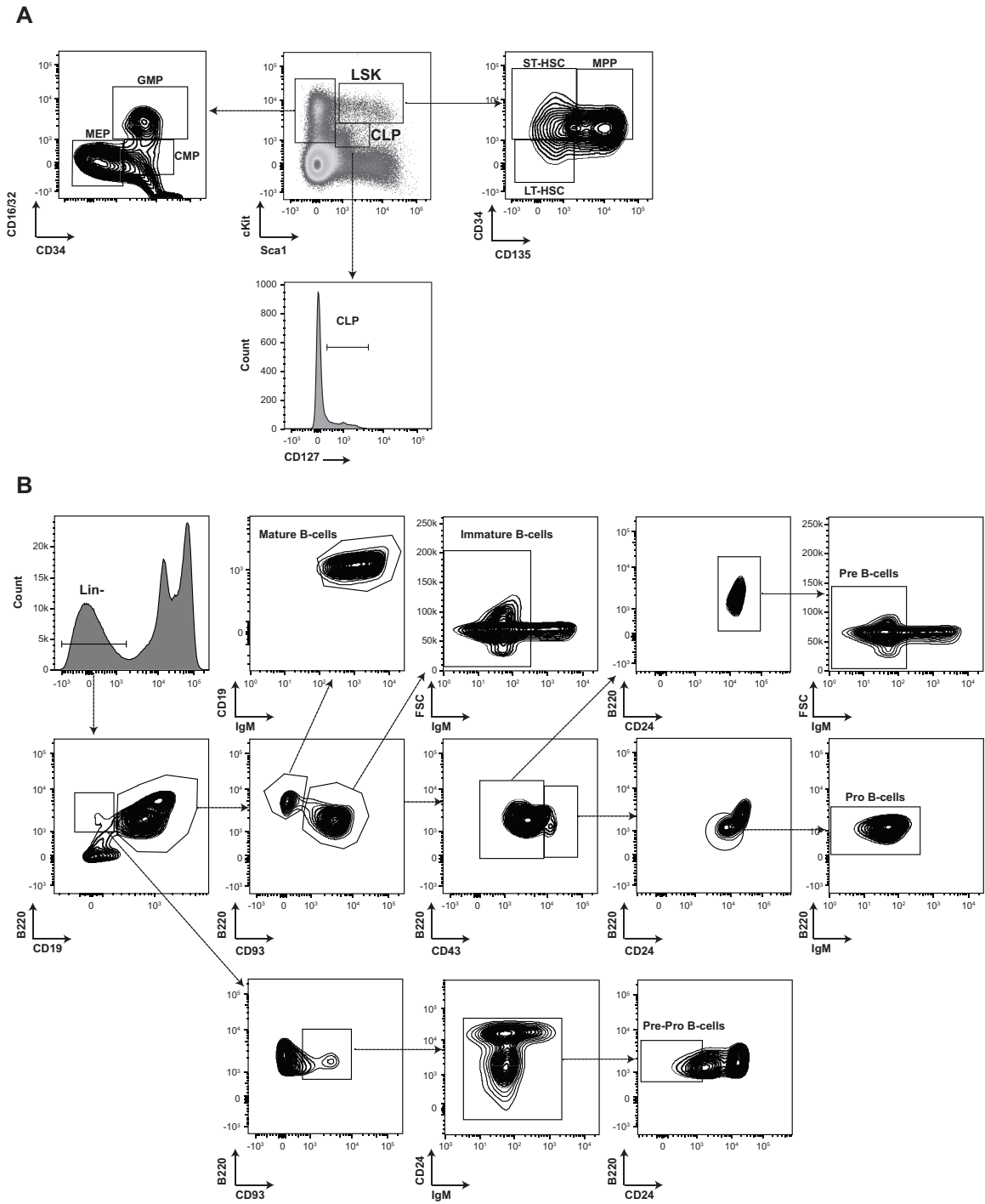


Figure S2. Gating strategies to identify hematopoietic stem/progenitor cells and B-cell precursor populations

(A) Exemplary flow cytometric gating strategy to identify hematopoietic stem and progenitor cells. Live bone marrow cells were stained with antibodies against Sca-1, ckit,

CD34, CD16/32 and CD127. Gating strategy for LSK population (Sca-1⁺ckit⁺) showing LT-HSC (CD135⁻CD34⁻), ST-HSC (CD135⁻CD34⁺) and MPP (CD135⁺CD34⁺). More differentiated progenitors gated in the LS⁻K⁺ population were sub-sectioned based on CD16/32 and CD34 expression to compare CMP, GMP and MEP progenitors. The CLP fraction, gated on LS^{low}K^{low}, is further gated on CD127 expression. LSK; Lineage⁻Sca-1⁺ckit⁺ population, LT-HSC; long-term hematopoietic stem cells, ST-HSC; short-term hematopoietic stem cells, MPP; multi-potent progenitors, CLP; common lymphoid progenitors, CMP; common myeloid progenitors, MEP; megakaryocyte-erythroid progenitors, GMP; granulocyte-macrophage progenitors.

(B) To determine the frequency of B-cell precursor populations, live bone marrow cells were stained with lineage markers, Sca-1, ckit, CD19, B220, CD93, IgM, CD43, and CD24. Gating strategies for selecting pre-pro-B-cells, pro-B-cells, pre-B -cells, immature B-cells and mature B-cells are shown.

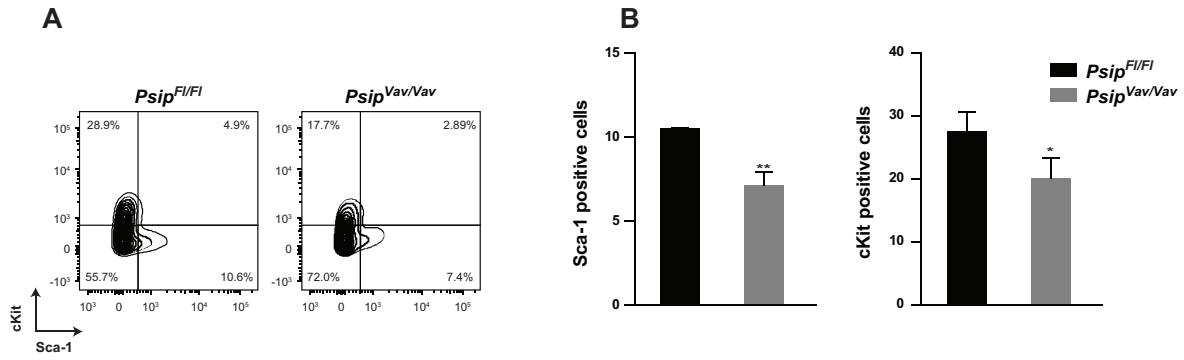


Figure S3. *Psip1* deletion alters the differentiation of HSC after CFU culture.

(A) Representative FACS analysis for Sca-1 and cKit expression in *Psip^{F1/F1}* and *Psip^{Vav/Vav}* cells, harvested after one round in myeloid CFU assay.

(B) Percentage of Sca-1 and cKit positive cells harvested after one round in myeloid CFU assay from 6 independent experiments. Mean values and SEM are indicated.

Significant differences were determined using Student's t-test; * $p < 0.05$, ** $p < 0.01$.

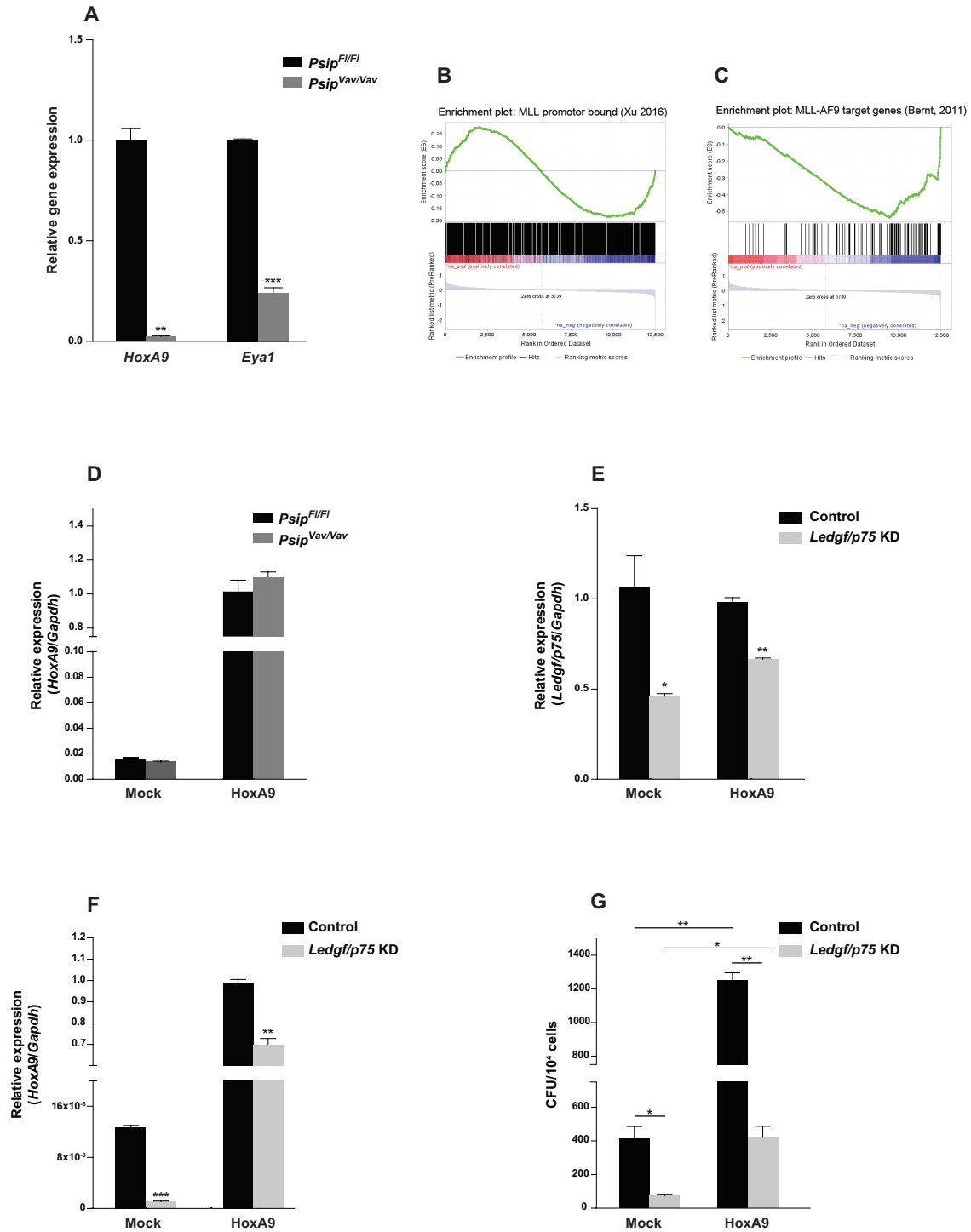


Figure S4. *HoxA9* overexpression rescues the defective colony formation in LEDGF/p75-deficient cells.

(A) qRT-PCR validation of known MLL target genes that are downregulated in *Psip*^{Vav/Vav} cells. Expression levels were normalized to *Gapdh*.

(B-C) Gene set enrichment analysis (GSEA) showing the correlation between the principle signature of the *Psip*^{Vav/Vav} samples and genes with promoter regions bound by wild-type MLL (B) and MLL-AF9 fusion (C).

(D) qRT-PCR measuring *HoxA9* expression levels (normalized to *Gapdh*) in *Psip*^{F1/F1} or *Psip*^{Vav/Vav} cells after transduction with a retroviral vector expressing *HoxA9* or a mock control.

(E-F) mRNA expression levels of *Ledgf/p75* (E) and *HoxA9* (F) from lin- cells of C57BL/6 mice transduced with lentiviral vector to knockdown (KD) *Ledgf/p75* or control and a retroviral vector expressing *HoxA9* or a mock control. Expression levels are normalized to *Gapdh*.

(G) CFU assay for *Ledgf/p75* knockdown or control cells after transduction with pMSCV-*HoxA9*-pgk-neo or mock vector.

Error bars represent standard deviation of triplicate measurements. Significant differences were determined using Student's t-test; * $p < 0.05$, ** $p < 0.01$, *** $p < 0.001$.

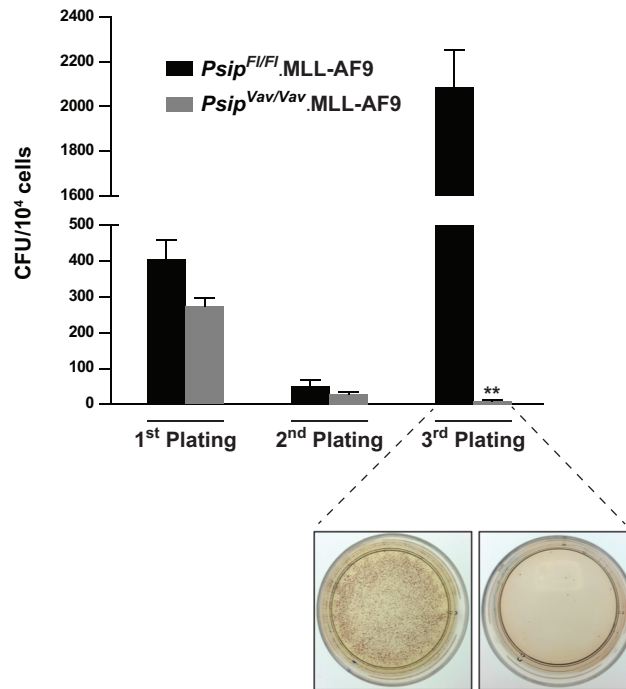


Figure S5. LEDGF/p75 is important for MLL-rearranged transformation

Three rounds of colony-forming units (CFU) per 10^4 *Psip*^{F1/F1} or *Psip*^{Vav/Vav} lin- cells transduced with a retroviral vector expressing *MLL-AF9* fusion. Representative images of the Tetrazolium-stained colonies after the third plating are shown. Error bars represent standard deviation of triplicate measurements. Statistical differences (** $p < 0.01$) were determined using Student's t-test.

Table S1. Primers used in this study.

Genotyping Primers	Sequence 5'-3'
mPSIP2331	GAGATATCGAGGCAGAAAGAAGACTGGGATAG
mPSIP2334	TGG AAT TCTATCTCAAACAAACCAAAGAGC
Vav-Cre_s	CTCTGACAGATGCCAGGACA
Vav-Cre_as	TGATTTTCAGGGATGGACACA

PCR Primers	Sequence 5'-3'
MLL_s	CGCCTCAGCCACCTACTACA
ENL_as	CCGGCAGCCTCCTCGCCT

qRT- PCR primers	Sequence 5'-3'
mPSIP2624	CCTCAAACATGACTCGCGATTTC
mPSIP2625	GCTCCATCAGGAACTTCATCTAC
mPSIP probe	AGACCTCATCTTCGCCAAGA
HoxA4_s	TGTACCCCTGGATGAAGAAGATC
HoxA4_as	GCTTAGGTTTCGCTCCGTTA
HoxA7_s	TATGTGAACGCGCTTTTTAGCA
HoxA7_as	GGGGGCTGTTGACATTGTATAA
HoxA9_s	GAA TGA GAG CGGCGGAGAC
HoxA9_as	GAGCGAGCATGTAGCCAGTTG
HoxA10_s	ACACTGGAGCTGGAGAAGGA
HoxA10_as	TCACTTGTCTGTCCGTGAGG
HoxA11_s	TTTGATGAGCGTGGTCCCTG
HoxA11_as	AGGAGTAGGAGTATGTCATTGGG
HoxB4_s	ATCTGTCTTGTTTCCTCTGCCG
HoxB4_as	TGAATGGGCACGAAAGATGAGG
HoxB8_s	TGATTTGTTGTGAGGCAAGAGA
HoxB8_as	CCATTAGAGACCCCGCATCC
Meis1_s	CCTCGGTCAATGACGCTTTAA
Meis1_as	GGTACAAGTAGCTAATTCACATTTCTC
Eya1_s	TCTCAGGTTTCAGCTCTCGGA
Eya1_as	GGGGTAGGGAGAATATGTGGG

Gapdh_s	TGTGTCCGTCGTGGATCTGA
Gapdh_as	CCTGCTTCACCACCTTCTTGA
Gapdh probe	CCGCCTGGAGAAACCTGCCAAGTATG

ChIP Primers	Sequence 5'-3'
HoxA9_s	GATACCAGAGCGGTTTCATACAG
HoxA9_as	TCGCCAGTCAACATCAAGAG
HoxA7_s	TAACCTGTCCGCCCAAAGAT
HoxA7_as	GCTGGAGCATCAAATCAGGTCT
β actin_s	AGCTTCTTTGCAGCTCCTT
β actin_as	TGAGGTACTAGCCACGAGAG

Table S2. FACS staining of hematopoietic progenitors in BM.

Laser	Channel	Antibody Target - Fluorochrome	Company	Dilution	
Blue 488nm 100mW	B-SSC	SSC			
	B-PE-Cy5-5	B-PE	CD135-PE	eBioscience	1/100
		CD3e-biotin	eBioscience	3/100	
		CD11b-biotin	eBioscience	3/100	
		B220-biotin	eBioscience	3/100	
		Ly-6G-biotin	eBioscience	3/100	
		Ter-119-biotin	eBioscience	3/100	
		Strep-PerCP-Cy5-5	eBioscience	1/100	
B-PE-Cy7	Ly-6A (Sca-1)-PE-Cy7	BD Pharmingen	1/200		
Violet 405nm 100mW	V-Pacific Blue	CD127-eFluor450	eBioscience	1/100	
	V-Amcyan	L/D-eFluor506	eBioscience	1/200	
Red 633nm 70mW	R-APC	CD34-eFluor660	eBioscience	1/200	
	R-AlexaFluor700	CD16/32-AlexaFluor 700	eBioscience	1/200	
	R-APC-Cy7	CD117 (c-Kit)-eFluor780	eBioscience	1/100	

Table S3. FACS staining of B-cell precursors in BM.

Laser	Channel	Antibody Target- Fluorochrome	Company	Dilution
Blue 488nm 50mW	B-SSC	SSC		
	B-FITC	IgM-FITC	BD Pharmingen	1/200
Violet 405nm 50mW	V-Pacific Blue	CD24-Pacific Blue	eBioscience	1/100
	V-Amcyan	L/D-eFluor506	eBioscience	1/200
	V-BV605	B220-BV605	eBioscience	1/200
Red 633nm 70mW	R-APC	CD93-APC	eBioscience	1/50
	R-APC-Cy7	CD19-APC-Cy7	BD Pharmingen	1/200
Yellow-Green 561nm 50mW	G-PE-TexasRed	CD127-PE-CF594	BD Pharmingen	1/100
	G-PE-Cy5	Ter119-PE-Cy5	eBioscience	1/200
	G-PE-Cy5	Gr1-PE-Cy5	eBioscience	1/200
	G-PE-Cy5	CD3-PE-Cy5	Tonbo Bioscience	1/200
	G-PE-Cy5	NK1.1-PE-Cy5	Biolegend	1/200
	G-PE-Cy5	CD11b-PE-Cy5	eBioscience	1/200
	G-PE-Cy7	CD43-PE-Cy7	Biolegend	1/100

Table S4. Differentially regulated genes ($p < 0.05$) between $Psip^{F1/F1}$ and $Psip^{Vav/Vav}$ cells.

Gene Symbol	Log2 Fold Change	P value
Ifi202b	-3.7710	4.95E ⁻¹⁵
Ctse	-3.2932	9.19E ⁻¹⁸
Gm9025	-3.2229	1.14E ⁻¹⁴
Hoxa9	-2.5245	1.88E ⁻⁰⁷
Ceacam2	-2.0396	1.55E ⁻⁰⁵
Psip1	-2.0350	5.85E ⁻¹¹
Cldn11	-2.0334	5.72E ⁻⁰⁶
Rps24-ps3	-2.0240	2.95E ⁻⁰⁵
Gm8822	-1.8563	1.24E ⁻⁰⁴
Psmas8	-1.5806	9.68E ⁻⁰⁴
Ptk7	-1.5397	7.71E ⁻⁰⁵
Eya1	-1.5321	1.58E ⁻⁰³
Mcpt1	-1.4934	1.66E ⁻⁰³
C1qa	-1.4531	1.98E ⁻⁰³
Rpsa-ps10	-1.4530	2.75E ⁻⁰⁴
Mcpt2	-1.4349	1.72E ⁻⁰³
Mcpt4	-1.4272	2.10E ⁻⁰³
St8sia1	-1.3811	3.71E ⁻⁰³
Capn11	-1.3765	4.02E ⁻⁰³
Gm13736	-1.3746	2.08E ⁻⁰³
F13a1	-1.2618	8.57E ⁻⁰⁴
1700006J14Rik	-1.1880	1.40E ⁻⁰²
Itln1	-1.1778	1.30E ⁻⁰³
Six1	-1.0811	1.34E ⁻⁰²
Slc26a9	-1.0663	2.50E ⁻⁰²
Hnmt	-1.0599	5.35E ⁻⁰³
Gm16754	-1.0422	3.14E ⁻⁰²
Gm1840	-1.0374	2.85E ⁻⁰²
Kcnip3	-1.0372	1.88E ⁻⁰²
Adgrl4	-0.9742	2.06E ⁻⁰²
Hoxa7	-0.9732	2.42E ⁻⁰²
Rgs13	-0.9726	2.83E ⁻⁰²
Gjb3	-0.9679	4.39E ⁻⁰²
Msl3l2	-0.9279	4.87E ⁻⁰²
Mef2c	-0.8897	6.67E ⁻⁰³

Gene Symbol	Log2 Fold Change	P value
Msantd3	-0.8773	3.49E ⁻⁰²
Ifi47	-0.8488	2.90E ⁻⁰²
Selenbp1	-0.8361	3.55E ⁻⁰²
Ankrd37	-0.8252	2.45E ⁻⁰²
Egln3	-0.8076	2.71E ⁻⁰²
Cox4i2	-0.7628	4.32E ⁻⁰²
2810417H13Rik	-0.7280	2.16E ⁻⁰²
Nphs2	-0.6443	2.60E ⁻⁰²
Gpr65	-0.6080	4.83E ⁻⁰²
Lmna	0.5855	3.42E ⁻⁰²
Slc6a4	0.5978	3.54E ⁻⁰²
Lztf11	0.6342	4.21E ⁻⁰²
Commd10	0.6506	2.23E ⁻⁰²
Rpl21-ps9	0.7047	4.24E ⁻⁰²
Ptprs	0.7476	8.66E ⁻⁰³
Rxra	0.7481	2.24E ⁻⁰²
BC100530	0.7605	4.29E ⁻⁰²
Ighg2c	0.7643	2.20E ⁻⁰²
Tmtc2	0.7682	3.78E ⁻⁰²
Inpp11	0.7774	4.17E ⁻⁰²
Bahcc1	0.7791	3.19E ⁻⁰²
Slc39a2	0.7821	3.96E ⁻⁰²
4931429I11Rik	0.7979	4.58E ⁻⁰²
Stfa3	0.8061	2.30E ⁻⁰²
Spats2	0.8179	3.75E ⁻⁰²
Zfp182	0.8298	4.92E ⁻⁰²
Kctd15	0.8317	4.39E ⁻⁰²
Gfra1	0.8384	4.94E ⁻⁰²
4931408C20Rik	0.8390	2.90E ⁻⁰²
Col27a1	0.8514	5.04E ⁻⁰²
Dok7	0.8550	1.31E ⁻⁰²
BC117090	0.8584	4.21E ⁻⁰²
Gabbr1	0.8641	3.89E ⁻⁰²
Gm10440	0.8650	1.67E ⁻⁰²
Gm4076	0.8684	3.91E ⁻⁰²

Fam213a	0.8686	3.66E ⁻⁰²	Rnf225	0.9810	4.13E ⁻⁰²
Lama5	0.8764	4.71E ⁻⁰²	Ephx1	0.9817	1.48E ⁻⁰²
Tmem98	0.8795	3.16E ⁻⁰²	Col23a1	0.9853	2.86E ⁻⁰³
Camkk1	0.8824	3.91E ⁻⁰²	Clefl	0.9855	2.69E ⁻⁰²
Gm5416	0.8837	1.31E ⁻⁰²	Epha2	0.9856	3.95E ⁻⁰²
Gprc5b	0.8868	4.51E ⁻⁰²	Ffar4	0.9858	2.15E ⁻⁰²
Mapre3	0.8933	4.46E ⁻⁰²	Kcnc3	0.9895	1.94E ⁻⁰²
Ckb	0.8957	4.34E ⁻⁰²	Crtam	0.9922	3.43E ⁻⁰²
Gem	0.8980	5.04E ⁻⁰²	Cacna1a	0.9949	2.77E ⁻⁰²
Igha	0.9001	2.74E ⁻⁰²	Fzd1	1.0020	1.92E ⁻⁰²
Adgrb2	0.9019	1.74E ⁻⁰²	Wwtr1	1.0028	3.58E ⁻⁰²
Rpp25	0.9067	4.55E ⁻⁰²	Rap1gap	1.0030	2.49E ⁻⁰²
Kenn3	0.9109	3.38E ⁻⁰²	Ptk2	1.0043	7.43E ⁻⁰³
Nipal4	0.9123	4.05E ⁻⁰²	Gm11410	1.0065	1.86E ⁻⁰²
Gm15663	0.9124	4.73E ⁻⁰²	Sh2d1b1	1.0072	1.17E ⁻⁰³
Tmem82	0.9143	1.52E ⁻⁰²	Slc9a5	1.0164	1.40E ⁻⁰²
Igf1	0.9165	1.42E ⁻⁰²	Slamf9	1.0226	1.10E ⁻⁰²
Akr1b8	0.9180	2.57E ⁻⁰²	Cacnb3	1.0249	3.39E ⁻⁰²
Ifi2712a	0.9207	4.33E ⁻⁰²	Gm37145	1.0253	2.08E ⁻⁰²
Serpnb6b	0.9225	4.21E ⁻⁰²	4930486L24Rik	1.0268	2.38E ⁻⁰²
Fam83h	0.9229	2.43E ⁻⁰²	Mmp25	1.0273	2.08E ⁻⁰²
Fbxw10	0.9250	4.76E ⁻⁰²	Cdkn2a	1.0284	2.22E ⁻⁰²
5830415G21Rik	0.9264	2.19E ⁻⁰²	Ugt8a	1.0299	3.30E ⁻⁰²
Tdrkh	0.9302	2.41E ⁻⁰²	Rhbdf1	1.0319	2.71E ⁻⁰²
Fam209	0.9328	4.52E ⁻⁰²	Trp53i11	1.0341	3.20E ⁻⁰²
Mn1	0.9423	3.75E ⁻⁰²	2900041M22Rik	1.0345	3.20E ⁻⁰²
Ccbe1	0.9443	2.59E ⁻⁰²	Tmem181c-ps	1.0351	3.07E ⁻⁰²
Mfsd7c	0.9453	4.92E ⁻⁰²	Npy	1.0437	7.63E ⁻⁰³
Pald1	0.9478	9.09E ⁻⁰⁴	Dcbld1	1.0444	2.55E ⁻⁰²
Pkp2	0.9483	8.90E ⁻⁰³	Adgrb1	1.0483	2.72E ⁻⁰²
Asb4	0.9520	3.88E ⁻⁰²	Dnah6	1.0492	2.96E ⁻⁰²
Tcf7l2	0.9562	2.24E ⁻⁰²	Ctsk	1.0508	1.26E ⁻⁰³
Trnp1	0.9576	4.69E ⁻⁰²	Sfmbt2	1.0540	2.92E ⁻⁰²
Myrf	0.9608	1.32E ⁻⁰²	Spred3	1.0614	1.54E ⁻⁰²
Slc9a2	0.9608	3.01E ⁻⁰²	Mrgpra4	1.0653	2.74E ⁻⁰²
Fat3	0.9614	4.36E ⁻⁰²	E230016M11Rik	1.0708	1.85E ⁻⁰²
Serpina3f	0.9670	4.54E ⁻⁰²	Unc13b	1.0774	9.44E ⁻⁰³
Snord19	0.9670	4.43E ⁻⁰²	Trim29	1.0855	2.08E ⁻⁰²
Ccdc40	0.9684	3.23E ⁻⁰²	Lyplal1	1.0866	2.06E ⁻⁰²
Khdrbs3	0.9723	4.09E ⁻⁰²	1700030C10Rik	1.0891	1.34E ⁻⁰²

Myo15b	0.9744	3.03E ⁻⁰²
Rpgrip1	1.0990	1.68E ⁻⁰²
Klk8	1.1023	1.83E ⁻⁰²
Plet1	1.1039	1.61E ⁻⁰²
Amigo2	1.1051	1.21E ⁻⁰²
Ptpn	1.1091	1.98E ⁻⁰²
Fabp7	1.1100	2.12E ⁻⁰²
Cfap45	1.1169	9.52E ⁻⁰³
Map1a	1.1179	2.02E ⁻⁰²
Meg3	1.1203	1.09E ⁻⁰²
Ush1c	1.1266	1.87E ⁻⁰²
Mrgprc2-ps	1.1313	1.36E ⁻⁰²
Tgfa	1.1336	1.05E ⁻⁰²
Bcam	1.1352	1.01E ⁻⁰²
Gm12648	1.1408	1.62E ⁻⁰²
Dsc2	1.1420	1.16E ⁻⁰²
Wtip	1.1440	1.74E ⁻⁰²
Neol	1.1480	1.05E ⁻⁰²
Slc12a5	1.1483	1.42E ⁻⁰²
Cftr	1.1487	1.69E ⁻⁰²
Fgf7	1.1502	1.38E ⁻⁰²
Chd5	1.1588	7.74E ⁻⁰³
Gm23301	1.1618	1.38E ⁻⁰²
Slc29a4	1.1665	1.22E ⁻⁰²
Deaf1211	1.1708	6.15E ⁻⁰³
Gm37068	1.1711	2.46E ⁻⁰³
Naip5	1.1737	1.05E ⁻⁰²
Gm13453	1.1857	1.38E ⁻⁰²
Scarf2	1.2222	7.48E ⁻⁰³
Zfp462	1.2322	7.05E ⁻⁰³
B930095G15Rik	1.2451	2.15E ⁻⁰³
Mal2	1.2485	7.34E ⁻⁰³

Rundc3a	1.0919	1.19E ⁻⁰²
Rbms3	1.4104	3.43E ⁻⁰³
Marco	1.2570	1.68E ⁻⁰³
Pls3	1.2650	1.30E ⁻⁰³
Shank1	1.2973	7.30E ⁻⁰³
Vangl1	1.3004	6.77E ⁻⁰³
3830403N18Rik	1.3122	5.23E ⁻⁰³
Adra2c	1.3383	4.86E ⁻⁰³
Arnt2	1.3393	2.18E ⁻⁰⁴
Mest	1.3740	3.79E ⁻⁰³
Peg12	1.3855	1.62E ⁻⁰⁴
Zfp467	1.3894	2.77E ⁻⁰³
Phf21b	1.4758	1.63E ⁻⁰³
Meis3	1.5136	2.57E ⁻⁰⁴
Kif21a	1.5277	2.08E ⁻⁰⁴
Ric3	1.5407	1.31E ⁻⁰³
H2afy2	1.5483	1.14E ⁻⁰³
Astn2	1.5594	1.24E ⁻⁰³
Fgfr1	1.5867	7.47E ⁻⁰⁵
Ccnd1	1.5969	1.07E ⁻⁰⁶
Arhgef26	1.6595	3.14E ⁻⁰⁴
Prickle2	1.7605	6.12E ⁻⁰⁵
Gm10093	1.7646	2.35E ⁻⁰⁴
Sva	2.0288	5.74E ⁻⁰⁶
Xkr6	2.0625	7.37E ⁻⁰⁷
Peg3	2.0971	5.29E ⁻⁰⁶
Fzd8	2.1279	8.67E ⁻⁰⁶
Uchl1	2.2424	9.70E ⁻⁰⁷
Adamts1	2.2802	2.37E ⁻⁰⁷
Ndn	2.3723	4.30E ⁻⁰⁷
Elavl2	2.4723	2.75E ⁻⁰⁷
Abcc8	2.8601	8.00E ⁻⁰¹¹

References

1. Méreau H, De Rijck J, Čermáková K, et al. Impairing MLL-fusion gene-mediated transformation by dissecting critical interactions with the lens epithelium-derived growth factor (LEDGF/p75). *Leukemia*. 2013;27(6):1245–1253.
2. Sun D, Melegari M, Sridhar S, Rogler C, Zhu L. Multi-miRNA hairpin method that improves gene knockdown efficiency and provides linked multi-gene knockdown. *BioTechniques*. 2006;41(1):59–63.
3. Milne TA, Zhao K, Hess JL. Chromatin immunoprecipitation (ChIP) for analysis of histone modifications and chromatin-associated proteins. *Methods Mol. Biol.* 2009;538(Chapter 21):409–423.
4. Dobin A, Davis CA, Schlesinger F, et al. STAR: ultrafast universal RNA-seq aligner. *Bioinformatics*. 2013;29(1):15–21.
5. Love MI, Huber W, Anders S. Moderated estimation of fold change and dispersion for RNA-seq data with DESeq2. *Genome Biology*. 2014;15(12):550.
6. Edgar R, Domrachev M, Lash AE. Gene Expression Omnibus: NCBI gene expression and hybridization array data repository. *Nucleic Acids Research*. 2002;30(1):207–210.
7. Wang Q-F, Wu G, Mi S, et al. MLL fusion proteins preferentially regulate a subset of wild-type MLL target genes in the leukemic genome. *Blood*. 2011;117(25):6895–6905.
8. Bernt KM, Zhu N, Sinha AU, Vempati S, Faber J. MLL-rearranged leukemia is dependent on aberrant H3K79 methylation by DOT1L. *Cancer Cell*. 2011.